Convergence acceleration techniques in CAD systems for grounding analysis in layered soils

I. Colominas, J. París, F. Navarrina, M. Casteleiro

Group of Numerical Methods in Engineering GMNI
Universidade da Coruña, SPAIN
email → icolominas@udc.es

Abstract

In the last years the authors have developed a numerical formulation based on the Boundary Element Method for the analysis of grounding systems embedded in uniform soils. This approach has been implemented in a CAD system that currently allows to analyze real grounding grids in real-time in personal computers. The extension of this approach for the grounding analysis in layered soils is straightforward by application of the method of images. However in some practical cases the resulting series have a poor rate of convergence; consequently, the analysis of real earthing grids in multilayer soils requires an out of range computational cost.

In this paper we present a CAD system based on this BEM numerical formulation for grounding analysis in multilayer soils that include an efficient technique based on the Aitken acceleration in order to improve the rate of convergence of the involved series expansions. Finally, we show some examples by using the geometry of real grounding systems.

Keywords: grounding, multilayer soils, BEM, acceleration convergence

1 Introduction

From the beginnings of the large-scale use of electricity, one of the challenging problems stated have been to obtain the potential distribution in electrical installations when a fault current is derived into the soil through a grounding system. Traditionally the grounding system refers to the earthing or grounding grid or the "grounded electrode" as its main element, being the potential distribution on the earth surface the most important parameter that it is necessary to know in order to design a safe grounding system.

In practice, the grounding grid usually consists of a mesh of interconnected cylindrical conductors buried to a certain depth of the ground surface ($0.5 - 1.0$ m), and supplemented by ground rods vertically thrusted in certain places of the substation site. Thus, when a fault condition occurs, the grounding grid transports and dissipates the electrical currents produced into the ground, with the aim of ensuring that a person in the vicinity of the grounded installation is not exposed to a critical electrical shock, and also preserving the continuity of the power supply and the integrity of the equipment. To achieve these goals, the equivalent electrical resistance of the system must be low enough to assure that fault currents dissipate mainly through the grounding grid into the earth. Moreover, electrical potential values between close points on the earth surface that can be connected by a person must be kept under certain maximum safe limits (step, touch and mesh voltages) [1, 2].

In the last four decades, several methods and procedures for the analysis and design of grounding grids have been proposed: methods based on the professional experience, on semi-empirical works, on experimental data obtained from scale model assays and laboratory tests, and even on intuitive ideas. Unquestionably, these contributions represented an important improvement in the grounding analysis area, although some problems have been systematically reported: the large computational costs required in the analysis of real cases, the unrealistic results obtained when segmentation of conductors is increased, and the uncertainty in the margin of error [1, 2, 3, 4], among others.

Maxwell's Electromagnetic Theory constitutes the starting point to obtain the mathematical equations that govern the dissipation of electrical currents into a soil. Nevertheless, although these equations are well-known for years, their application and resolution for the computing of grounding grids of large installations in practical cases present serious difficulties. First, it is obvious that no analytical solutions can be obtained for most of real problems. On the other hand, the characteristic geometry of grounding systems (a mesh of interconnected bare conductors with a relatively small ratio diameter-length) makes very difficult the use of numerical methods. Thus, the use of some widespread numerical techniques commonly applied for solving boundary value problems in engineering, such as finite elements or finite differences, is extremely costly since it is required the discretization of the domain: the ground excluding the electrode. Consequently, obtaining sufficiently accurate results should imply unacceptable computing efforts in memory storage and CPU time.

In the last years, the authors have developed a numerical formulation based on the Boundary Element Method for the analysis of grounding systems with uniform soil models[5, 6]. Its implementation in a Computer Aided Design application for grounding systems allows to analyze real grounding installations in real-time using conventional personal computers.

Later, we proposed a generalization of the boundary element formulation for grounding grids embedded in layered soils [7, 8]. This is a very challenging problem with important consequences in the grounding design from the safety point of view [1]. These stratified soil models are frequently used when there are important differences

in the electrical properties of the soil: for example, when the excavation process during the construction of the substation produces a layered soil, or as a consequence of a chemical treatment of the soil applied in the surroundings of the earthing system to improve the performance of the grounding electrode, or due to the specific geological characteristics of the substation site.

However the analysis of real grounding grids in multilayer soils requires in some practical cases an out-of-range computational cost due to the poor rate of convergence of the series that appear when the method of images is applied to represent the different layers of soil. This topic becomes the bottleneck of the whole numerical approach. In this paper we focus our attention on this problem proposing the use of an efficient and mathematically well-founded extrapolation technique in order to accelerate the rate of convergence of the involved series expansions.

2 Math model of the current dissipation problem

2.1 General equations

The dissipation of electrical currents into the soil can be studied in the framework of the Maxwell's Electromagnetic Theory. If one restricts the analysis to the electrokinetic steady-state response and neglects the inner resistivity of the earthing conductors (so, potential is assumed constant at every point of the grounding electrode surface), the 3D problem can be written as

$$\begin{gathered} \operatorname{div}(\boldsymbol{\sigma}) = 0, \quad \boldsymbol{\sigma} = -\boldsymbol{\gamma}\,\mathbf{grad}(V) \text{ in } E; \\ \boldsymbol{\sigma}^t \boldsymbol{n}_E = 0 \text{ in } \Gamma_E; \;\; V = V_\Gamma \text{ in } \Gamma; \;\; V \to 0, \text{ if } |\boldsymbol{x}| \to \infty \end{gathered} \tag{1}$$

where E is the earth, $\boldsymbol{\gamma}$ is its conductivity tensor, Γ_E is the earth surface, $\boldsymbol{n}_E$ is its normal exterior unit field and Γ is the electrode surface [5]. Therefore, the solution to (1) gives potential V and current density $\boldsymbol{\sigma}$ at an arbitrary point $\boldsymbol{x}$ when the electrode attains a voltage V_Γ (Ground Potential Rise, or GPR) with respect to remote earth. Next, for known values of V on Γ_E and $\boldsymbol{\sigma}$ on Γ, it is straightforward to obtain the design and safety parameters of the grounding system [5, 9]. On the other hand, since V and $\boldsymbol{\sigma}$ are proportional to the GPR value [5], from here on it will be used the normalized boundary condition $V_\Gamma = 1$.

The most commonly soil model considered in many of the methods proposed for grounding analysis is the homogeneous and isotropic one, where conductivity $\boldsymbol{\gamma}$ is substituted by an apparent scalar conductivity γ [1, 5]. Obviously, this hypothesis is valid (and it does not introduce significant errors) if the soil is "essentially uniform" in all directions in the surroundings of the grounding grid; this model can even be used with loss of accuracy if the soil resistivity changes slightly with depth. Nevertheless, safety parameters involved in the grounding design can strongly vary if the soil electrical properties change through the substation site, particularly with the depth. These variations can be due to changes in the material nature, or in the humidity of the

soil, for example. For this reason, it is necessary to develop more advanced models to consider variations of the soil conductivity in the surroundings of the grounding site.

Obviously, taking into account all variations of soil conductivity would be meaningless and unaffordable, neither from the economical nor from the technical point of view. For this reason, more practical soil models have been proposed. A family of these soil models consists of assuming the soil stratified in a number of horizontal or vertical layers, defined by an appropriate thickness and an apparent scalar conductivity that must be experimentally obtained. In fact, it is widely accepted that two-layer and three-layer soil models should be sufficient to obtain good and safe designs of grounding systems in most practical cases[1].

In the hypothesis of a stratified soil model formed by C layers with different conductivities, the mathematical problem (1) can be written in terms of the following Neumann exterior problem

$$\begin{gathered}\operatorname{div}(\boldsymbol{\sigma}_c) = 0,\ \boldsymbol{\sigma}_c = -\gamma_c \operatorname{\mathbf{grad}}(V_c) \text{ in } E_c,\ 1 \leq c \leq C; \\ \boldsymbol{\sigma}_1^t \boldsymbol{n}_E = 0 \text{ in } \Gamma_E,\ V_b = 1 \text{ in } \Gamma; \\ V_c \to 0 \text{ if } |\boldsymbol{x}| \to \infty,\ \boldsymbol{\sigma}_c^t \boldsymbol{n}_c = \boldsymbol{\sigma}_{c+1}^t \boldsymbol{n}_c \text{ in } \Gamma_c,\ 1 \leq c \leq C-1;\end{gathered} \tag{2}$$

where b denotes the layer in which the grounded electrode is buried, E_c is each one of the soil layers, γ_c is its scalar conductivity, V_c is the potential at an arbitrary point in the layer E_c, $\boldsymbol{\sigma}_c$ is its corresponding current density, Γ_c is the interface between layers E_c and E_{c+1}, and $\boldsymbol{n}_c$ is the normal field to Γ_c[8]. In this paper we restrict the grounding analysis and examples for two-layer soil models, that is $C = 2$.

2.2 Integral Expression for Potential and Variational Form

The ratio between the diameter and the length of the conductors of the grounding grids uses to be relatively small ($\sim 10^{-3}$). This apparently simple geometry implies serious troubles in the modellization of the problem in real cases: neither analytical solutions can be obtained, nor widespread numerical methods (such as finite elements or finite differences) can be used since the required discretization of the 3D domains E_c (excluding the grounding electrode) should involve a completely out-of-range computing effort. For these reasons, we have turned our attention to other numerical techniques which require only the discretization of the boundaries. With this aim, it is firstly essential to derive an integral expression for potential V in terms of unknowns defined on the boundary[5, 9].

First of all, we can assumed that the earth surface Γ_E and the interfaces Γ_c between layers are horizontal (this hypothesis seems sound if we take into account the levelling and regularization processes performed in the surroundings of the substation site during the construction process of the electrical installation).

With this new assumption, the application of the "method of images" and Green's Identity to problem (2) yields the following integral expression[8] for potential $V_c(\boldsymbol{x}_c)$ at an arbitrary point $\boldsymbol{x}_c \in E_c$, in terms of the unknown leakage current density $\sigma(\boldsymbol{\xi})$

($\sigma = \boldsymbol{\sigma}^t \boldsymbol{n}$, where $\boldsymbol{n}$ is the normal exterior unit field to Γ) at any point $\boldsymbol{\xi}$ of the electrode surface $\Gamma \subset E_b$:

$$V_c(\boldsymbol{x_c}) = \frac{1}{4\pi\gamma_b} \int \int_{\boldsymbol{\xi}\in\Gamma} k_{bc}(\boldsymbol{x}_c, \boldsymbol{\xi})\, \sigma(\boldsymbol{\xi}) d\Gamma, \ \forall \boldsymbol{x}_c \in E_c, \tag{3}$$

where integral kernels $k_{bc}(\boldsymbol{x}_c, \boldsymbol{\xi})$ are formed by series of infinite terms corresponding to the resultant images obtained when Neumann exterior problem (2) is transformed into a Dirichlet one[5, 8, 9]. Depending on the type of the soil model, these series can have an infinite or a finite number of terms: i.e., for uniform soil models ($C = 1$), there are only two summands since there is only one image of the original grid:

$$k_{11}(\boldsymbol{x}_1, \boldsymbol{\xi}) = \frac{1}{r(\boldsymbol{x}_1, [\xi_x, \xi_y, \xi_z])} + \frac{1}{r(\boldsymbol{x}_1, [\xi_x, \xi_y, -\xi_z])}, \tag{4}$$

where $r(\boldsymbol{x}_1, [\xi_x, \xi_y, \xi_z])$ indicates the distance from $\boldsymbol{x}_1$ to $\boldsymbol{\xi} \equiv [\xi_x, \xi_y, \xi_z]$, being the point $[\xi_x, \xi_y, -\xi_z]$ the symmetric one of $\boldsymbol{\xi}$ with respect to the earth surface Γ_E. We assume that the origin of the coordinates system is on the earth surface and the z-axis is perpendicular to Γ_E.

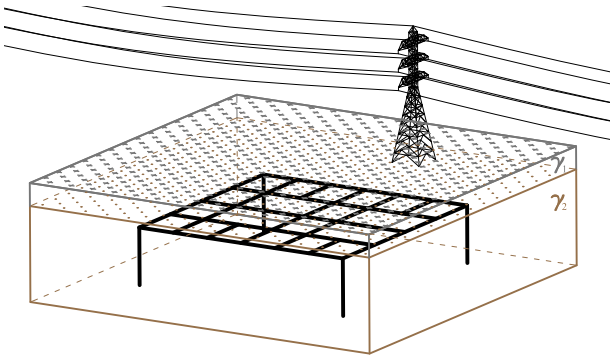

Figure 1: Scheme of a two-layer soil model formed by an upper layer with a thickness h and conductivity γ_1, and a lower layer with conductivity γ_2.

In the case of a two-layered soil model (figure 1), the expressions of the integral kernels $k_{bc}(\boldsymbol{x}_c, \boldsymbol{\xi})$ are given by

$$\begin{aligned}
k_{11} = &\sum_{i=0}^{\infty} \frac{\kappa^i}{r(\boldsymbol{x}_1, [\xi_x, \xi_y, 2iH + \xi_z])} + \sum_{i=0}^{\infty} \frac{\kappa^i}{r(\boldsymbol{x}_1, [\xi_x, \xi_y, 2iH - \xi_z])} \\
&+ \sum_{i=1}^{\infty} \frac{\kappa^i}{r(\boldsymbol{x}_1, [\xi_x, \xi_y, -2iH + \xi_z])} + \sum_{i=1}^{\infty} \frac{\kappa^i}{r(\boldsymbol{x}_1, [\xi_x, \xi_y, -2iH - \xi_z])}; \\
k_{12} = &\sum_{i=0}^{\infty} \frac{(1+\kappa)\kappa^i}{r(\boldsymbol{x}_2, [\xi_x, \xi_y, -2iH + \xi_z])} + \sum_{i=0}^{\infty} \frac{(1+\kappa)\kappa^i}{r(\boldsymbol{x}_2, [\xi_x, \xi_y, -2iH - \xi_z])}; \\
k_{21} = &\sum_{i=0}^{\infty} \frac{(1-\kappa)\kappa^i}{r(\boldsymbol{x}_1, [\xi_x, \xi_y, -2iH + \xi_z])} + \sum_{i=0}^{\infty} \frac{(1-\kappa)\kappa^i}{r(\boldsymbol{x}_1, [\xi_x, \xi_y, 2iH - \xi_z])};
\end{aligned}$$

$$k_{22}=\frac{1}{r(\boldsymbol{x}_2,[\xi_x,\xi_y,\xi_z])}-\frac{\kappa}{r(\boldsymbol{x}_2,[\xi_x,\xi_y,2H+\xi_z])}+\sum_{i=0}^{\infty}\frac{(1-\kappa^2)\kappa^i}{r(\boldsymbol{x}_2,[\xi_x,\xi_y,-2iH+\xi_z])}; \quad (5)$$

In the above expressions, $r(\boldsymbol{x},[\xi_x,\xi_y,\xi_z])$ indicates the distance from $\boldsymbol{x}$ to $\boldsymbol{\xi}$. The other terms correspond to the distances from $\boldsymbol{x}$ to the symmetric point of $\boldsymbol{\xi}$ with respect to the earth surface Γ_E, and to the interface surface between layers. H is the thickness of the upper layer. Ratio κ is defined in terms of the layer conductivities

$$\kappa=\frac{\gamma_1-\gamma_2}{\gamma_1+\gamma_2} \quad (6)$$

From expressions (4) and (5), it is clear that singular kernels $k_{bc}(\boldsymbol{x}_c,\boldsymbol{\xi})$ for uniform and two-layer soil models can be written in a general form

$$k_{bc}(\boldsymbol{x}_c,\boldsymbol{\xi})=\sum_{l=0}^{l_k}k_{bc}^{l}(\boldsymbol{x}_c,\boldsymbol{\xi}), \quad k_{bc}^{l}(\boldsymbol{x}_c,\boldsymbol{\xi})=\frac{\psi^l(\kappa)}{r(\boldsymbol{x}_c,\boldsymbol{\xi}^l(\boldsymbol{\xi}))}, \quad (7)$$

where ψ^l is a weighting coefficient that depends only on the ratio κ given by (6), and $r(\boldsymbol{x}_c,\boldsymbol{\xi}^l(\boldsymbol{\xi}))$ is the Euclidean distance between the points $\boldsymbol{x}_c$ and $\boldsymbol{\xi}^l$, being $\boldsymbol{\xi}^0$ the point $\boldsymbol{\xi}$ on the electrode surface ($\boldsymbol{\xi}^0(\boldsymbol{\xi})=\boldsymbol{\xi}$), and being $\boldsymbol{\xi}^l$ ($l\neq 0$) the images of $\boldsymbol{\xi}$ with respect to the earth surface and to the interfaces between layers. Finally, l_k is the number of summands in the series of integral kernels, and it depends on the case being analyzed.

On the other hand, expression (3) is very important for the solution of the problem since it allows to obtain the value of the electrical potential at an arbitrary point $\boldsymbol{x}_c$ if the leakage current density σ is known. Furthermore, it is also possible to compute the total surge current that flows from the grounding system, its equivalent resistance and most of the remaining safety and design parameters of a grounding grid [5]. The leakage current density σ can be obtained by solving the following Fredholm integral equation of the first kind on Γ

$$\frac{1}{4\pi\gamma_b}\iint_{\boldsymbol{\xi}\in\Gamma}k_{bb}(\boldsymbol{\chi},\boldsymbol{\xi})\sigma(\boldsymbol{\xi})\,d\Gamma=1, \qquad \forall\boldsymbol{\chi}\in\Gamma. \quad (8)$$

since the integral expression for the potential (3) is also satisfied on the electrode surface Γ, where the potential value is known by the boundary condition $V_b(\boldsymbol{\chi})=1$, $\forall\boldsymbol{\chi}\in\Gamma$. Now, a variational form of this integral expression can be obtained by imposing that it is verified in the sense of weighted residuals, that is, the following integral identity

$$\iint_{\boldsymbol{\chi}\in\Gamma}w(\boldsymbol{\chi})\left(\frac{1}{4\pi\gamma_b}\iint_{\boldsymbol{\xi}\in\Gamma}k_{bb}(\boldsymbol{\chi},\boldsymbol{\xi})\sigma(\boldsymbol{\xi})\,d\Gamma-1\right)d\Gamma=0, \quad (9)$$

must hold for all members $w(\boldsymbol{\chi})$ of a suitable class of test functions defined on Γ[5, 9]. It is important to remark that the solution of equation (8) only requires obtaining the leakage current density σ in points of the electrode surface. So, a numerical method based on the discretization of the boundaries of the domain, such as the BEM [5, 10], should be the best numerical approach for solving it.

3 Numerical model based on the BEM

3.1 General 2D approach

The unknown leakage current density σ and the electrode surface Γ can be discretized in terms of a given set of N trial functions $\{N_i(\boldsymbol{\xi})\}$ defined on Γ and a given set of M 2D boundary elements $\{\Gamma^\alpha\}$:

$$\sigma(\boldsymbol{\xi}) = \sum_{i=1}^{N} \sigma_i \, N_i(\boldsymbol{\xi}), \qquad \Gamma = \bigcup_{\alpha=1}^{M} \Gamma^\alpha, \tag{10}$$

Now, the integral expression (3) for the potential $V_c(\boldsymbol{x}_c)$ can also be discretized as

$$V_c(\boldsymbol{x}_c) = \sum_{i=1}^{N} \sigma_i V_{c,i}(\boldsymbol{x}_c); \;\; V_{c,i}(\boldsymbol{x}_c) = \sum_{\alpha=1}^{M} \sum_{l=0}^{l_V} V_{c,i}^{\alpha l}(\boldsymbol{x}_c); \tag{11}$$

$$V_{c,i}^{\alpha l}(\boldsymbol{x}_c) = \frac{1}{4\pi\gamma_b} \iint_{\boldsymbol{\xi}\in\Gamma^\alpha} k_{bc}^{l}(\boldsymbol{x}_c, \boldsymbol{\xi}) \, N_i(\boldsymbol{\xi}) \; d\Gamma^\alpha; \tag{12}$$

where l_V represents the number of summands to consider in the evaluation of the series of kernels until convergence is achieved ($l_V = l_k$ if this number is finite).

Finally, variational form (9) is reduced to the following LSE for a given set of N test functions $\{w_j(\boldsymbol{\chi})\}$ defined on Γ:

$$\begin{aligned} \sum_{i=1}^{N} R_{ji}\sigma_i = \nu_j \qquad & (j = 1, \ldots, N) \\ R_{ji} = \sum_{\beta=1}^{M}\sum_{\alpha=1}^{M}\sum_{l=0}^{l_R} R_{ji}^{\beta\alpha l}, \qquad & \nu_j = \sum_{\beta=1}^{M} \nu_j^\beta, \end{aligned} \tag{13}$$

being

$$R_{ji}^{\beta\alpha l} = \frac{1}{4\pi\gamma_b} \iint_{\boldsymbol{\chi}\in\Gamma^\beta} w_j(\boldsymbol{\chi}) \iint_{\boldsymbol{\xi}\in\Gamma^\alpha} k_{bb}^{l}(\boldsymbol{\chi}, \boldsymbol{\xi}) N_i(\boldsymbol{\xi}) d\Gamma^\alpha d\Gamma^\beta, \tag{14}$$

$$\nu_j^\beta = \iint_{\boldsymbol{\chi}\in\Gamma^\beta} w_j(\boldsymbol{\chi}) d\Gamma^\beta, \tag{15}$$

where l_R represents the number of summands to consider in the evaluation of the series of kernels until convergence is achieved ($l_R = l_k$ if this number is finite).

Solution of the linear system (12) provides the values of the current densities σ_i $(i = 1, \ldots, N)$ leaking from the nodes of the grid. However, In practice, the 2D discretization required to solve the above stated equations in real problems implies an extremely large number of degrees of freedom. In addition, the coefficient matrix in (13) is full and the computation of each contribution (14) requires double integration on a 2D domain[5, 9] and, in the case of kernels given by infinite series, an extremely high number of evaluations of terms of the kernel. For these reasons, it is essential to introduce some additional simplifications in the BEM approach to decrease the computational cost.

3.2 Approximated 1D BEM approach

With this aim, and taking into account the real geometry of grounding grids in most of electrical substations, one can assume that the leakage current density is constant around the cross section of the cylindrical electrode (hypothesis of "circumferential uniformity") [1, 5, 8].

Consequently, if we denote L the whole set of axial lines of the buried conductors, $\widehat{\boldsymbol{\xi}}$ the orthogonal projection over the bar axis of a given generic point $\boldsymbol{\xi} \in \Gamma$, $\phi(\widehat{\boldsymbol{\xi}})$ the electrode diameter, $P(\widehat{\boldsymbol{\xi}})$ the circumferential perimeter of the cross section in $\widehat{\boldsymbol{\xi}}$, and $\widehat{\sigma}(\widehat{\boldsymbol{\xi}})$ the approximated leakage current density at this point (assumed uniform around the cross section), we can derive an approximated expression for potential (3) as,

$$\widehat{V}_c(\boldsymbol{x}_c) = \frac{1}{4\gamma_b} \int_{\widehat{\boldsymbol{\xi}} \in L} \phi(\widehat{\boldsymbol{\xi}})\, \bar{k}_{bc}(\boldsymbol{x}_c, \widehat{\boldsymbol{\xi}})\, \widehat{\sigma}(\widehat{\boldsymbol{\xi}})\, dL, \quad \forall \boldsymbol{x}_c \in E_c \tag{16}$$

being $\bar{k}_{bc}(\boldsymbol{x}_c, \widehat{\boldsymbol{\xi}})$ the average of the integral kernel $k_{bc}(\boldsymbol{x}_c, \widehat{\boldsymbol{\xi}})$ in the cross section in $\widehat{\boldsymbol{\xi}}$:

$$\bar{k}_{bc}(\boldsymbol{x}_c, \widehat{\boldsymbol{\xi}}) = \int_{\boldsymbol{\xi} \in P(\widehat{\boldsymbol{\xi}})} k_{bc}(\boldsymbol{x}_c, \boldsymbol{\xi}) dP. \tag{17}$$

Now, the variational identity (9) will not hold, because the leakage current is not exactly uniform around the cross section and boundary condition $V_1(\boldsymbol{\chi}) = 1$, $\boldsymbol{\chi} \in \Gamma$ will not be strictly satisfied at every point $\boldsymbol{\chi}$ on Γ. For it, restricting the class of trial functions to those with circumferential uniformity (i.e., $w(\boldsymbol{\chi}) = \widehat{w}(\widehat{\boldsymbol{\chi}})\ \forall \boldsymbol{\chi} \in P(\widehat{\boldsymbol{\chi}})$), we obtain the new variational form

$$\frac{1}{4\gamma_b} \int_{\widehat{\boldsymbol{\chi}} \in L} \phi(\widehat{\boldsymbol{\chi}})\, \widehat{w}(\widehat{\boldsymbol{\chi}}) \left[\int_{\widehat{\boldsymbol{\xi}} \in L} \phi(\widehat{\boldsymbol{\xi}})\, \bar{\bar{k}}_{bb}(\widehat{\boldsymbol{\chi}}, \widehat{\boldsymbol{\xi}})\, \widehat{\sigma}(\widehat{\boldsymbol{\xi}})\, dL \right] dL = \int_{\widehat{\boldsymbol{\chi}} \in L} \phi(\widehat{\boldsymbol{\chi}})\, \widehat{w}(\widehat{\boldsymbol{\chi}})\, dL, \tag{18}$$

which it must be verified for all functions $\widehat{w}(\widehat{\boldsymbol{\chi}})$ of a suitable class of test ones defined on L, where integral kernel $\bar{\bar{k}}_{bb}(\widehat{\boldsymbol{\chi}}, \widehat{\boldsymbol{\xi}})$ is given by

$$\bar{\bar{k}}_{bb}(\widehat{\boldsymbol{\chi}}, \widehat{\boldsymbol{\xi}}) = \int_{\boldsymbol{\chi} \in P(\widehat{\boldsymbol{\chi}})} \left[\int_{\boldsymbol{\xi} \in P(\widehat{\boldsymbol{\xi}})} k_{bb}(\boldsymbol{\chi}, \boldsymbol{\xi})\, dP \right] dP. \tag{19}$$

In contrast to integral equation (9), the resolution of (18) requires the discretization of the whole set of axial lines L of the grounded conductors. Thus, the unknown approximated leakage current density $\widehat{\sigma}$ and the axial lines L can be discretized if we consider a set of n trial functions $\{\widehat{N}_i(\widehat{\boldsymbol{\xi}})\}$ defined on L, and a set of m 1D boundary elements $\{L^\alpha\}$:

$$\widehat{\sigma}(\widehat{\boldsymbol{\xi}}) = \sum_{i=1}^{n} \widehat{\sigma}_i\, \widehat{N}_i(\widehat{\boldsymbol{\xi}}), \qquad L = \bigcup_{\alpha=1}^{m} L^\alpha, \tag{20}$$

Now, it is possible to discretize the approximated potential (16)

$$\widehat{V}_c(\boldsymbol{x}_c) = \sum_{i=1}^{n} \widehat{\sigma}_i\, \widehat{V}_{c,i}(\boldsymbol{x}_c); \qquad \widehat{V}_{c,i}(\boldsymbol{x}_c) = \sum_{\alpha=1}^{m} \sum_{l=0}^{l_V} \widehat{V}_{c,i}^{\alpha l}(\boldsymbol{x}_c); \tag{21}$$

$$\widehat{V}_{c,i}^{\alpha l}(\boldsymbol{x}_c) = \frac{1}{4\gamma_b} \int_{\widehat{\boldsymbol{\xi}} \in L^\alpha} \phi(\widehat{\boldsymbol{\xi}})\, \bar{k}_{bc}^{l}(\boldsymbol{x}_c, \widehat{\boldsymbol{\xi}})\, \widehat{N}_i(\widehat{\boldsymbol{\xi}})\; dL^\alpha, \tag{22}$$

where l_V represents the number of summands to consider in the evaluation of the series of kernels until convergence is achieved ($l_V = l_k$ if this number is finite).

Finally, the variational form (18) is also reduced to a LSE for a given set of n test functions $\{\widehat{w}_j(\widehat{\boldsymbol{\chi}})\}$ defined on L:

$$\begin{gathered} \sum_{i=1}^{n} \widehat{R}_{ji} \widehat{\sigma}_i = \widehat{\nu}_j \qquad (j = 1, \ldots, n) \\ \widehat{R}_{ji} = \sum_{\beta=1}^{m} \sum_{\alpha=1}^{m} \sum_{l=0}^{l_R} \widehat{R}_{ji}^{\beta\alpha l}, \qquad \widehat{\nu}_j = \sum_{\beta=1}^{m} \widehat{\nu}_j^{\beta}, \end{gathered} \tag{23}$$

where

$$\widehat{R}_{ji}^{\beta\alpha l} = \frac{1}{4\gamma_b} \int_{\widehat{\boldsymbol{\chi}} \in L^\beta} \phi(\widehat{\boldsymbol{\chi}})\, \widehat{w}_j(\widehat{\boldsymbol{\chi}}) \int_{\widehat{\boldsymbol{\xi}} \in L^\alpha} \phi(\widehat{\boldsymbol{\xi}})\, \bar{\bar{k}}_{bb}^{l}(\widehat{\boldsymbol{\chi}}, \widehat{\boldsymbol{\xi}})\, \widehat{N}_i(\widehat{\boldsymbol{\xi}})\, dL^\alpha dL^\beta, \tag{24}$$

$$\widehat{\nu}_j^{\beta} = \int_{\widehat{\boldsymbol{\chi}} \in L^\beta} \phi(\widehat{\boldsymbol{\chi}})\, \widehat{w}_j(\widehat{\boldsymbol{\chi}})\, dL^\beta. \tag{25}$$

In contrast with the 2D boundary element general formulation, the number of elemental contributions needed to state the system of linear equations (23) and the number of unknowns σ_i are now significantly smaller for a given level of mesh refinement. In spite of the important reduction in the computational cost, extensive computing is still necessary mainly because of the circumferential integration on the perimeter of the electrodes that are involved in the integral kernels. In previous works we have proposed the approximated evaluation of these circumferential integrals by using specific quadratures [5]: thus, kernel (17) can be computed as

$$\bar{k}_{bc}(\boldsymbol{x}_c, \widehat{\boldsymbol{\xi}}) = \sum_{l=0}^{l_V} \bar{k}_{bc}^{l}(\boldsymbol{x}_c, \widehat{\boldsymbol{\xi}}) \tag{26}$$

being

$$\bar{k}_{bc}^{l}(\boldsymbol{x}_c, \widehat{\boldsymbol{\xi}}) = \pi\, \phi(\widehat{\boldsymbol{\xi}})\, \frac{\psi^l(\kappa)}{\widehat{r}(\boldsymbol{x}_c, \widehat{\boldsymbol{\xi}}^l(\widehat{\boldsymbol{\xi}}))}; \qquad \widehat{r}(\boldsymbol{x}_c, \widehat{\boldsymbol{\xi}}^l) = \sqrt{|\boldsymbol{x}_c - \widehat{\boldsymbol{\xi}}^l|^2 + \frac{\phi^2(\widehat{\boldsymbol{\xi}})}{4}} \tag{27}$$

and kernel (19) can be obtained as

$$\bar{\bar{k}}_{bb}(\widehat{\boldsymbol{\chi}}, \widehat{\boldsymbol{\xi}}) = \sum_{l=0}^{l_R} \bar{\bar{k}}_{bb}^{l}(\widehat{\boldsymbol{\chi}}, \widehat{\boldsymbol{\xi}}) \tag{28}$$

being

$$\bar{\bar{k}}_{bb}^{l}(\widehat{\boldsymbol{\chi}}, \widehat{\boldsymbol{\xi}}) = \pi^2\, \phi(\widehat{\boldsymbol{\xi}})\, \phi(\widehat{\boldsymbol{\chi}})\, \frac{\psi^l(\kappa)}{\widehat{\bar{r}}(\widehat{\boldsymbol{\chi}}, \widehat{\boldsymbol{\xi}}^l(\widehat{\boldsymbol{\xi}}))}; \qquad \widehat{\bar{r}}(\widehat{\boldsymbol{\chi}}, \widehat{\boldsymbol{\xi}}^l) = \sqrt{|\widehat{\boldsymbol{\chi}} - \widehat{\boldsymbol{\xi}}^l|^2 + \frac{\phi^2(\widehat{\boldsymbol{\xi}}) + \phi^2(\widehat{\boldsymbol{\chi}})}{4}} \tag{29}$$

The final result is an approximated 1D formulation in which the coefficients of the equations system only requires integration on 1D domains, i.e. the axial lines of the electrodes [5].

Different choices of the sets of trial and test functions allow to derive specific numerical approaches. In this paper, we have selected a Galerkin type one, where the matrix of coefficients is symmetric and positive definite [5, 9, 11]. On the other hand, the authors have derived a highly efficient analytical technique to evaluate the coefficients of the linear system of equations for Point Collocation and Galerkin type weighting in uniform soil models. Since the 1D approximated expressions for the terms $\widehat{V}_{c,i}^{\alpha l}$ and $\widehat{R}_{ji}^{\beta\alpha l}$ in (22) and (24) are formally equivalent to those obtained in the case of uniform soil models, their computation can also be performed analytically by using the above mentioned techniques [5, 9].

4 Convergence acceleration techniques of the series

Series involved in the calculus of kernels (26) and (28) have a poor rate of convergence particularly when the ratio κ —given by (6)— is close to +1 or -1; that is, when there are important differences between the electrical properties of the two layers of soil: these are the most interesting cases. It is important to remark that the increase in the computing cost by the use of multilayer soil models is justified when conductivities drastically vary since two-layer (or in general multilayer) models produce results noticeably different from those obtained by using a uniform soil model.

Kernels (26) and (28) appear in the computing of potential terms (21) and in the computing of matrix coefficients terms (23). Of course, both terms are important and the series involved in each computations have a similar rate of convergence. However in practice computing potential distribution on the earth surface usually is the bottleneck of the complete process of grounding analysis, since it is necessary to compute the potential in an extremely high number of points on the earth surface in order to obtain high-quality results and to compute the safety parameters of the grounding grid: for a substation site of an approximated area of 40.000 m^2 it is necessary to compute the value of potential in approximately 50.000 points by using formula (21). If we take into account that expression (21) can also be rewritten as

$$\widehat{V}_c(\boldsymbol{x}_c) = \sum_{l=0}^{l_V} \left(\sum_{i=1}^{n} \widehat{\sigma}_i \sum_{\alpha=1}^{m} \widehat{V}_{c,i}^{\alpha l}(\boldsymbol{x}_c) \right) \tag{30}$$

where l_V represents the number of summands to consider in the evaluation of the series of kernels until convergence is achieved, it is clear that obtaining potential distribution on earth surface could break off the design process due to the scale factor of the number of points if $l_V >> 1$. For this reason we have focused our attention to develop a technique for accelerate the convergence of the series involved in the potential values computing.

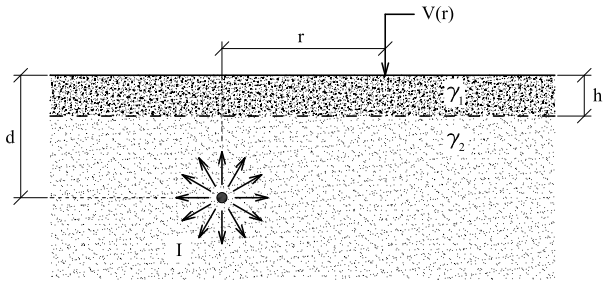

Figure 2: Scheme of a punctual source of current with intensity I buried to a depth d in a two-layer soil formed by an upper layer with a thickness h and conductivity γ_1, and a lower layer with conductivity γ_2.

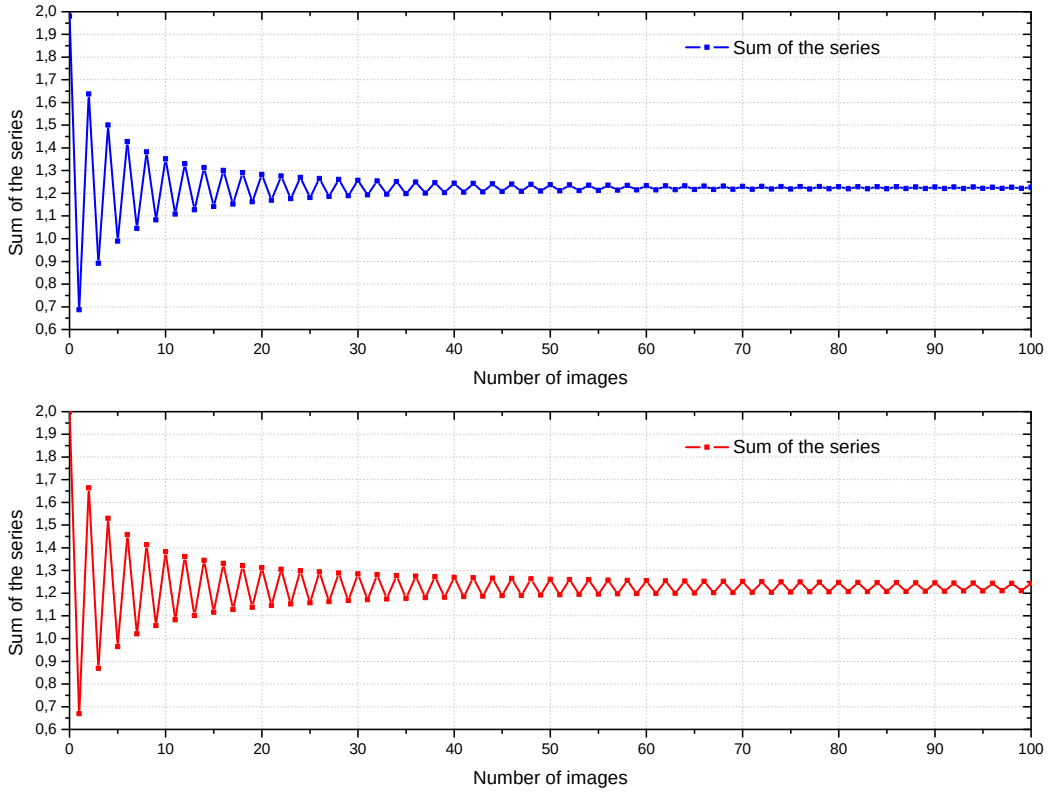

Figure 3: Potential on earth surface produced by a punctual current source buried to a depth d in a two-layer soil of thickness of the upper layer h ($d > h$): Results depending on the number of images computed for a $\kappa = -0.98$ (in blue) and $\kappa = -0.998$ (in red) for a ratio $\widetilde{r} = 0$ (point on the earth surface over the vertical of the punctual source) and $\widetilde{h} = 0.25$.

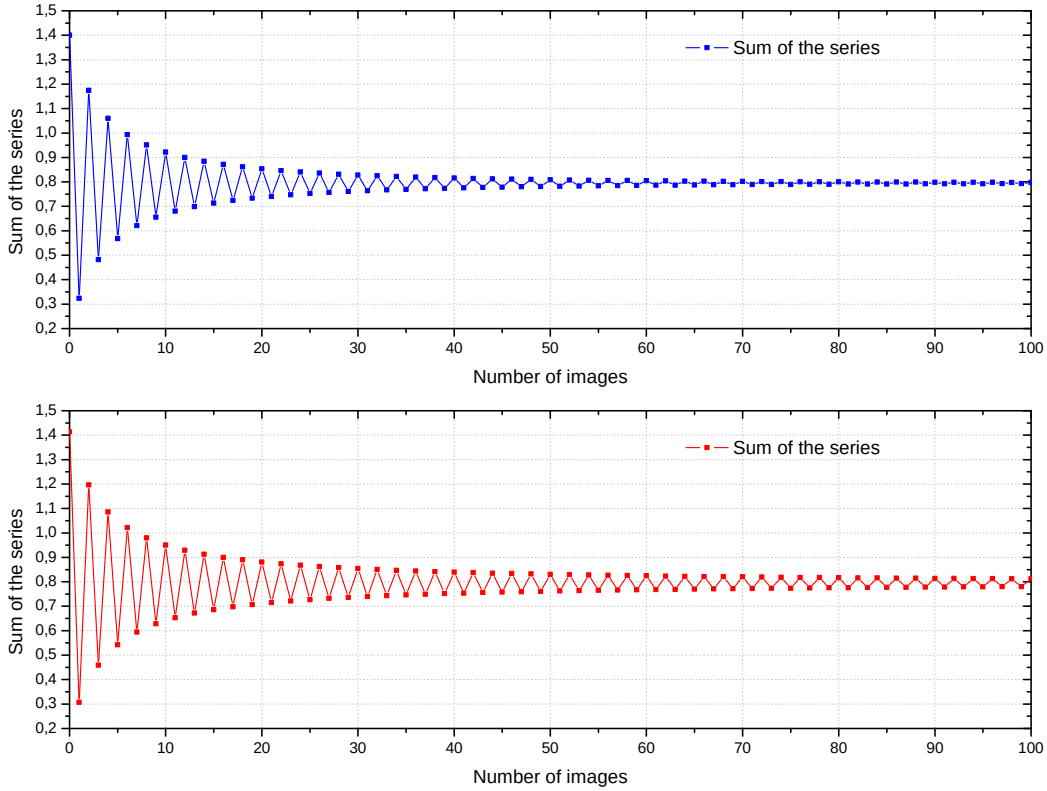

Figure 4: Potential on earth surface produced by a punctual current source buried to a depth d in a two-layer soil of thickness of the upper layer h ($d > h$): Results depending on the number of images computed for a $\kappa = -0.98$ (in blue) and $\kappa = -0.998$ (in red) for a ratio $\widetilde{r} = 1$ (point on the earth surface to a distance d over the vertical of the punctual source) and $\widetilde{h} = 0.25$.

4.1 Convergence of the potential calculus in the case of a punctual current source

The starting point in the derivation of our proposal for acceleration of the convergence of the series consists in studyng the upper bound of the error when the potential is computed in the ground surface. Thus, let be a punctual source of current with intensity I buried to a depth d in a two-layer soil formed by an upper layer with a thickness h and conductivity γ_1, and a lower layer with conductivity γ_2 (Figure 2).

The potential V on the ground surface is given by the following two expressions depending on the position of the source[12, 13, 14]: If it is placed in the upper layer, then $d < h$, and potential is given by

$$V(r) = \frac{I}{2\pi d\gamma_1}\left(\frac{1}{\sqrt{\widetilde{r}^2+1}} + \sum_{n=1}^{\infty}\left[\frac{\kappa^n}{\sqrt{\widetilde{r}^2+(2n\widetilde{h}-1)^2}} + \frac{\kappa^n}{\sqrt{\widetilde{r}^2+(2n\widetilde{h}+1)^2}}\right]\right); \tag{31}$$

being $\widetilde{r} = r/d$ and $\widetilde{h} = h/d$. If the punctual source is in the lower layer, then $d > h$, and potential is given by

$$V(r) = \frac{I}{2\pi d\gamma_2} \sum_{n=0}^{\infty} \frac{(1-\kappa)\kappa^n}{\sqrt{\widetilde{r}^2 + (2n\widetilde{h}+1)^2}}; \tag{32}$$

Figures 3 and 4 shows the potential (32) for two different situations. The values of the parameters have been chosen similar to real geometric configurations: i.e., $\widetilde{h} = h/d = 0.25$ corresponds to $d = 1$ m and $h = 0.25$ m, $\kappa = -0.98$ corresponds to the case of $\gamma_1 = 10^{-4}$ mho/m and $\gamma_2 = 10^{-2}$ mho/m, and $\kappa = -0.998$ corresponds to the case of $\gamma_1 = 10^{-5}$ mho/m and $\gamma_2 = 10^{-2}$ mho/m. (The value of intensity I has been chosen $I = 2\pi d\gamma_2$ in order to represent directly the series in all graphics).

In both formulae, κ is the ratio between conductivities, given by (6).

Now if we denote ε_N the absolute error produced in the calculus of the potential by computing N terms of the series (that is, by using the first N images), then it is given by $\varepsilon_N = V - V^N$, being V the exact value and V^N the approximation by computing N terms:

$$\varepsilon_N = V - V^N = \frac{I}{2\pi d\gamma_1} \sum_{n=N}^{\infty} \left[\frac{\kappa^n}{\sqrt{\widetilde{r}^2 + (2n\widetilde{h}-1)^2}} + \frac{\kappa^n}{\sqrt{\widetilde{r}^2 + (2n\widetilde{h}+1)^2}} \right]; \text{if } \; d < h \tag{33}$$

This error is upper bounded by

$$|\varepsilon_N| < \left| \frac{I}{\pi d\gamma_1} \frac{(1-\kappa)\kappa^N}{\sqrt{\widetilde{r}^2 + (2\widetilde{h}-1)^2}} \right|; \text{if } \; d < h \tag{34}$$

and consequently the common-logarithm of $|\varepsilon_N|$ is linear dependent with N

$$\log|\varepsilon_N| < \log|A| + N\log|\kappa|; \;\; \text{if } \; d < h \tag{35}$$

where A depends on geometric parameters, and it is a constant value for every potential calculus. If $d > h$, the absolute error is given by

$$\varepsilon_N = V - V^N = \frac{I}{2\pi d\gamma_2} \sum_{n=N}^{\infty} \frac{(1-\kappa)\kappa^n}{\sqrt{\widetilde{r}^2 + (2n\widetilde{h}+1)^2}}; \;\; \text{if } \; d > h \tag{36}$$

and its upper bound is

$$|\varepsilon_N| < \left| \frac{I}{2\pi d\gamma_2} \frac{\kappa^N}{\sqrt{\widetilde{r}^2 + (2\widetilde{h}+1)^2}} \right|; \text{if } \; d > h \tag{37}$$

and consequently the common logarithm of $|\varepsilon_N|$ is again linear dependent with N

$$\log|\varepsilon_N| < \log|B| + N\log|\kappa|; \;\; \text{if } \; d > h \tag{38}$$

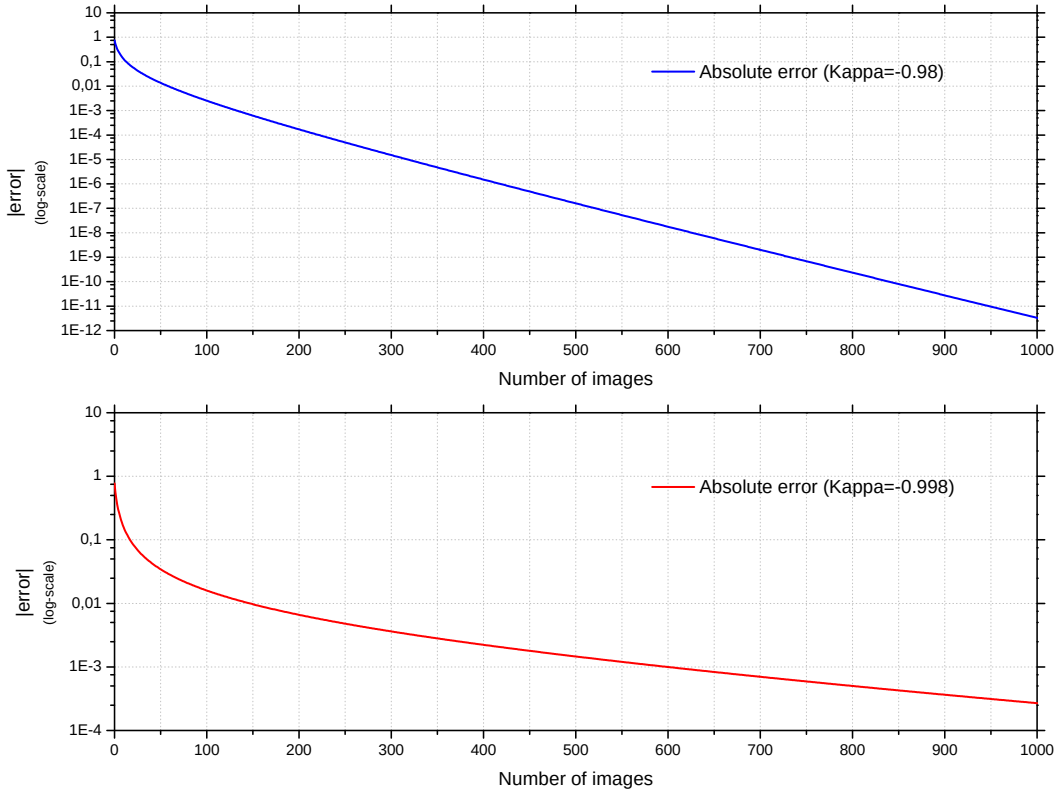

Figure 5: Absolute error in the potential computing on earth surface produced by a punctual current source buried to a depth d in a two-layer soil of thickness of the upper layer h ($d > h$): Results depending on the number of images computed for a $\kappa = -0.98$ (in blue) and $\kappa = -0.998$ (in red) for ratios $\widetilde{r} = 0$ and $\widetilde{h} = 0.25$.

where B depends on geometric parameters, and it is a constant value for every potential calculus. Figures 5 and 6 shows the evolution of absolute error in the computation of potential —expression (36)— for different cases. The linear dependency of the log-error is clear when the number of images increases as predicted by formulae (37) and (38).

As we can observe from expressions (35) and (38), the upper bound of the absolute error (in logarithmic scale) is linear with N. Both are very important results. If the potential is computed by using two different numbers of terms of the series (namely N_1, N_2), the Richardson extrapolation allows to conclude that $\varepsilon_{N_2} = \varepsilon_{N_1}\kappa^{(N_2-N_1)}$, that is, a geometric convergence is achieved since $|\kappa| < 1$. This expression is useful to obtain *extrapolated values* for the electrical potential (V^E). For example, if $N_2 = N_1 + 1$ then

$$V^E = \frac{V^{N_2} - \kappa V^{N_1}}{1 - \kappa} \tag{39}$$

Furthermore, and due to this geometric convergence, the Aitken acceleration can also be used to obtain an *improved value of potential*, by using the computed values of

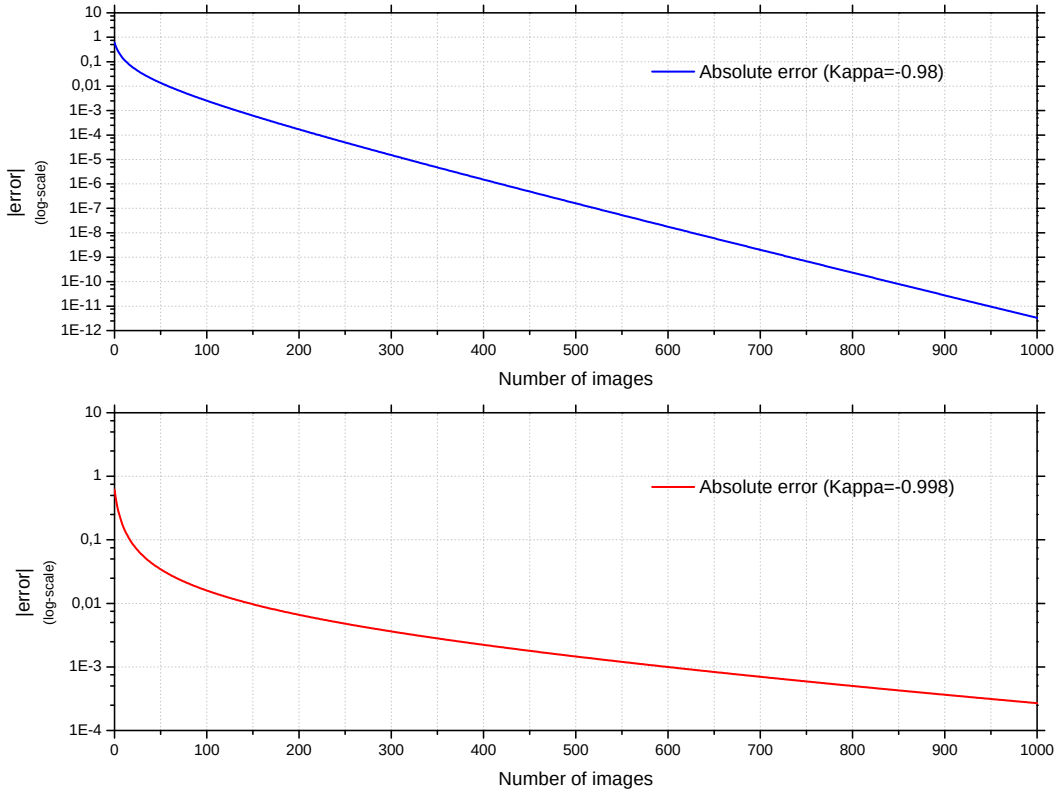

Figure 6: Absolute error in the potential computing on earth surface produced by a punctual current source buried to a depth d in a two-layer soil of thickness of the upper layer h ($d > h$): Results depending on the number of images computed for a $\kappa = -0.98$ (in blue) and $\kappa = -0.998$ (in red) for ratios $\widetilde{r} = 1$ and $\widetilde{h} = 0.25$.

the potential with three different numbers of terms of the series (namely N_1, N_2 and N_3, satisfying $N_1 < N_2 < N_3$ and $N_3 - N_2 = N_2 - N_1$, being V^{N_1}, V^{N_2} and V^{N_3} the computed values for each case). Thus, the Aitken acceleration allows to obtain a expression for computing an *improved value of potential* ($V^\star$):

$$V^\star = \frac{V^{N_1}V^{N_3} - V^{N_2}V^{N_2}}{V^{N_1} + V^{N_3} - 2V^{N_2}} \tag{40}$$

This formula is very simple and easy to use: for a given point on the ground surface, three values of the potential (32) should be computed by using N_1, N_2 and N_3 number of terms of the series (for example, with 5, 10 and 15 images) and then it is computed the *improved* value $V^\star$ by using the Aitken acceleration given by (40). Figures 7 and 8 shows the potential values and the extrapolated potential ones versus the number of images. It is important to remark the good quality of the extrapolated values obtained with a few number of images. (As in the previous graphics, the value of intensity I has been chosen $I = 2\pi d\gamma_2$ in order to represent directly the series).

Figures 9 and 10 shows the number of images necessary to compute the potential if

no extrapolation is used versus the number of images if extrapolation is used. It is also represented the relative error in the potential value. Note that the number of images required would be extremely specially when $|\kappa| \approx 1$ (i.e., $\kappa = -0.998$) where the rate of convergence of the series is very poor.

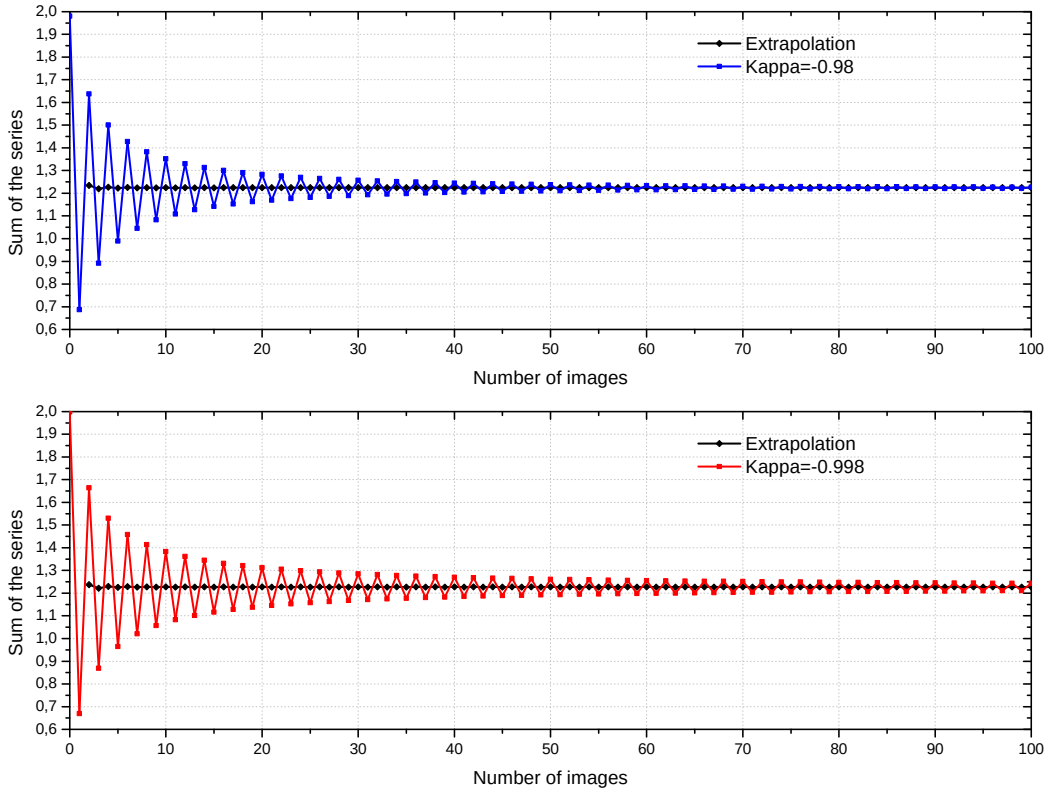

Figure 7: Potential values and *potential improved* values by using the Aitken acceleration (40) on earth surface produced by a punctual current source buried to a depth d in a two-layer soil of thickness of the upper layer h ($d > h$) computed for a $\kappa = -0.98$ (in blue) and $\kappa = -0.998$ (in red) for ratios $r/d = 0$ and $h/d = 0.25$.

4.2 Application of the convergence acceleration of the series to the grounding analysis by the Boundary Element Method

The idea presented in the previous section was the starting point for developing a more efficient computational way for obtaining potential in layered soil models. In the numerical approach based on the Boundary Element Method, the absolute error (ε_N) produced in the calculus of the potential by using expression (30) and computing N terms of the series, it is given by $\varepsilon_N = \widehat{V}_c^{\infty}(\boldsymbol{x}_c) - \widehat{V}_c^{N}(\boldsymbol{x}_c)$, being $\widehat{V}_c^{\infty}(\boldsymbol{x}_c)$ the exact

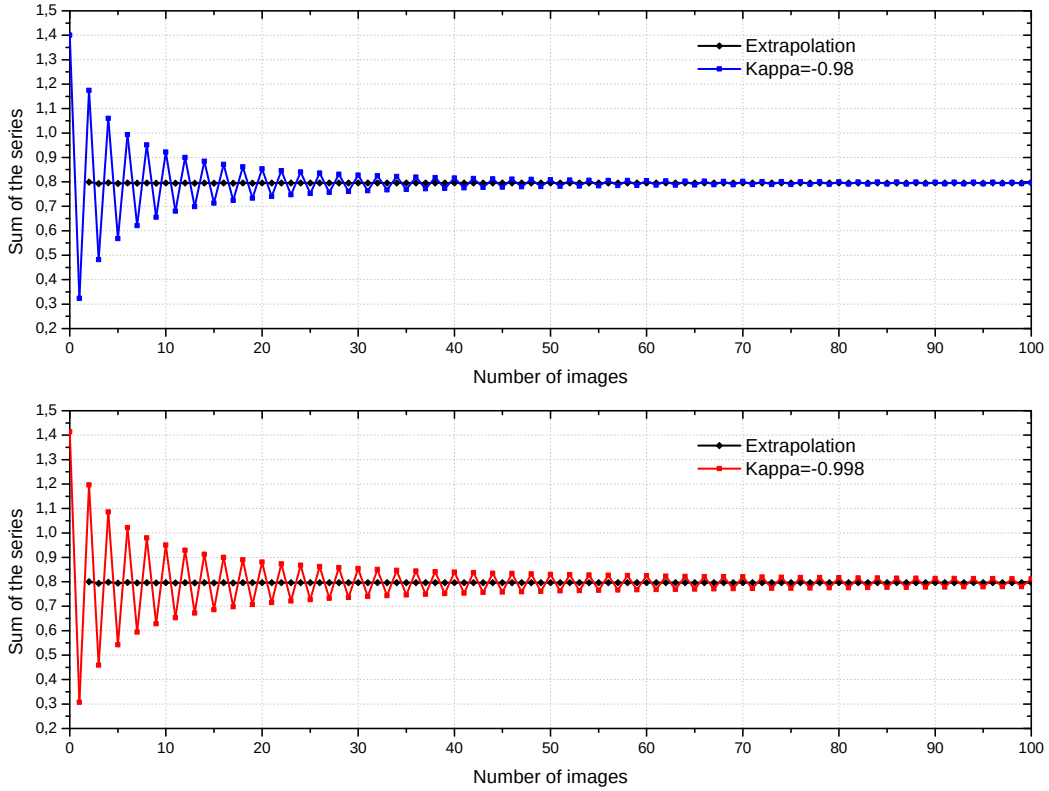

Figure 8: Potential values and *potential improved* values by using the Aitken acceleration (40) on earth surface produced by a punctual current source buried to a depth d in a two-layer soil of thickness of the upper layer h ($d > h$) computed for a $\kappa = -0.98$ (in blue) and $\kappa = -0.998$ (in red) for ratios $r/d = 1$ and $h/d = 0.25$.

value and $\widehat{V}_c^N(\boldsymbol{x}_c)$ the approximation by computing N terms:

$$\varepsilon_N = \widehat{V}_c^{\infty}(\boldsymbol{x}_c) - \widehat{V}_c^N(\boldsymbol{x}_c) = \sum_{l=N}^{\infty} \left(\sum_{i=1}^{n} \widehat{\sigma}_i \sum_{\alpha=1}^{m} \widehat{V}_{c,i}^{\alpha l}(\boldsymbol{x}_c) \right) \tag{41}$$

Now substituting (22) and (27) in (41), it is possible to rewrite the previous expression as

$$\varepsilon_N = \widehat{V}_c^{\infty}(\boldsymbol{x}_c) - \widehat{V}_c^N(\boldsymbol{x}_c) = \sum_{l=N}^{\infty} \psi^l(\kappa) \Phi_c^l(\boldsymbol{x}_c) \tag{42}$$

where $\Phi_c^l(\boldsymbol{x}_c)$ represents the contribution to the potential calculus of the image l (it is important to remark that $\Phi_c^l(\boldsymbol{x}_c)$ is not a function of κ). Finally it can be shown the upper bound of the absolute error is given by an expression of the form

$$|\varepsilon_N| < \left| \Psi \kappa^N \right| \tag{43}$$

where Ψ depends on geometric parameters, and it is a constant value for every potential calculus. This result is formally equivalent to the one obtained in the study of the

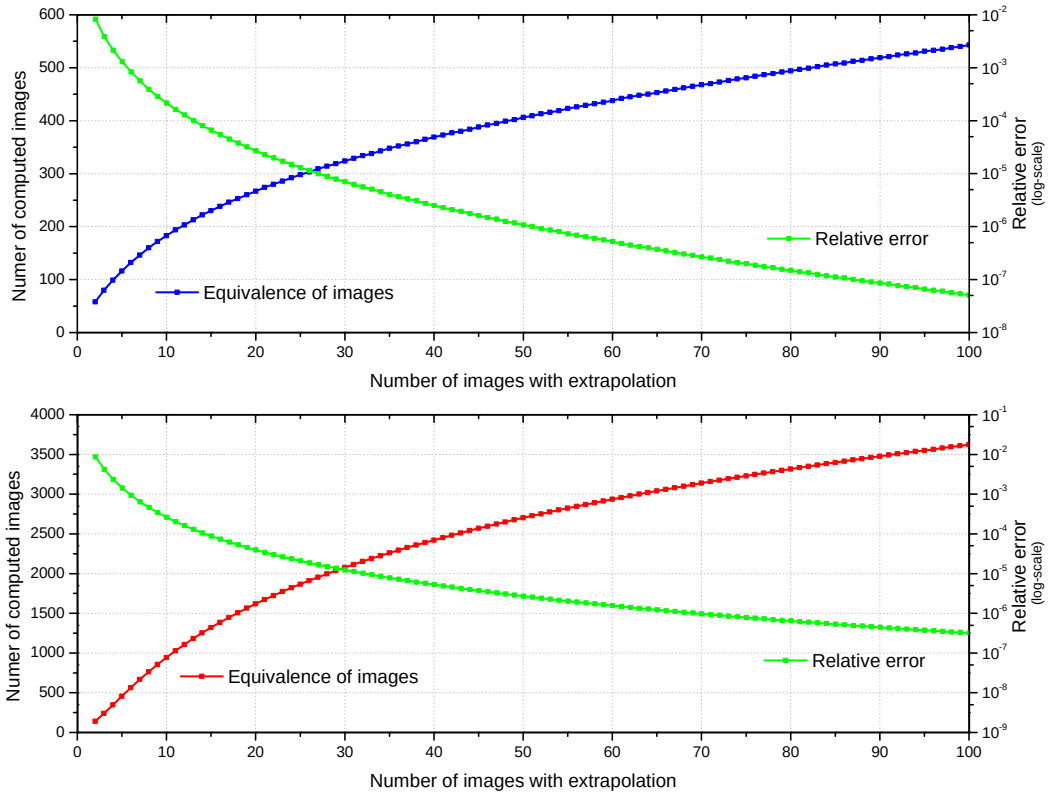

Figure 9: Number of images versus the number of images necessary for *potential improved* values by using the Aitken acceleration (40) on earth surface produced by a punctual current source buried to a depth d in a two-layer soil of thickness of the upper layer h ($d > h$) computed for a $\kappa = -0.98$ (in blue) and $\kappa = -0.998$ (in red) for ratios $r/d = 0$ and $h/d = 0.25$. It is also represented the potential relative error.

punctual source (and given by (37)), so we can use expression the Aitken acceleration given by (40) to obtain *improved* values of the potential.

This methodology of computing interpolated values of the potential has been implemented in the Computer Aided Design system for grounding analysis based on the approach proposed in sections 2. and 3. and based on the Boundary Element Method. Consequently, the computation of potential by using expression (21) is programmed in such way as new terms of the series (corresponding to new images) are added, the *improved* values are also computed. The rise of computational cost due to this extra-calculus is completely irrelevant and the convergence is quickly achieved.

The improvement in the rate of convergence of the series is remarkably and the CPUtime required in the postprocessing stage of the grounding analysis of a real case is reduced in a factor of two orders of magnitude on average for two-layer soil models of κ very closer to -1.

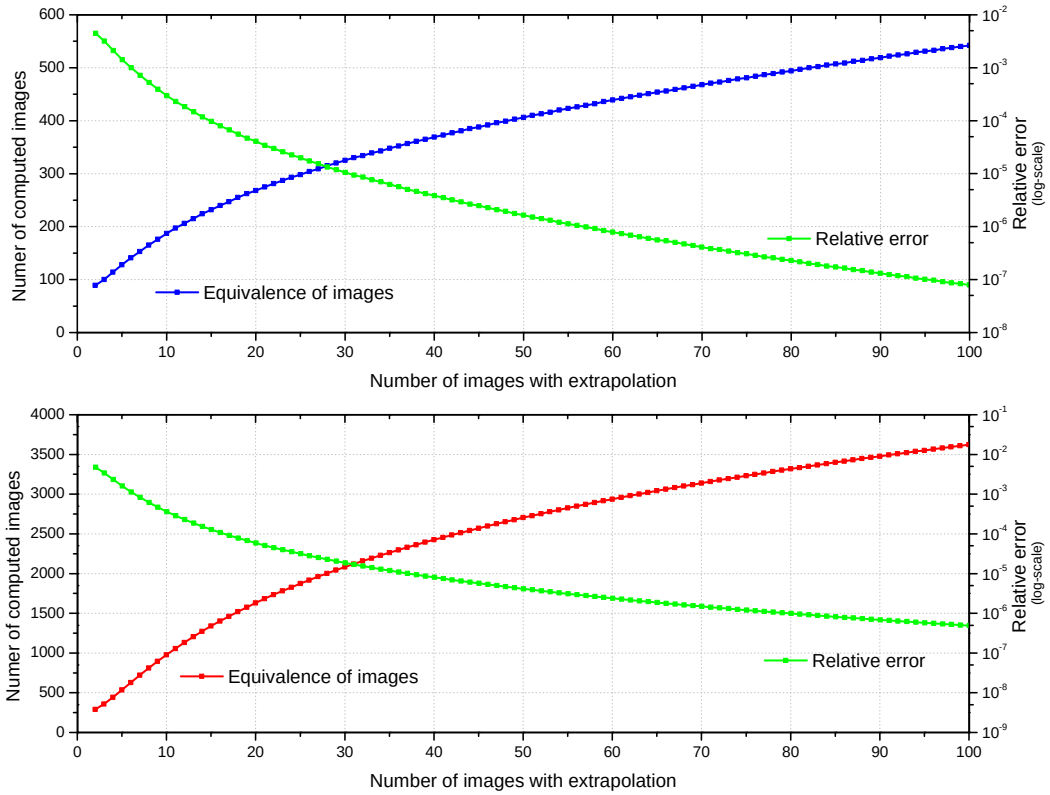

Figure 10: Number of images versus the number of images necessary for *potential improved* values by using the Aitken acceleration (40) on earth surface produced by a punctual current source buried to a depth d in a two-layer soil of thickness of the upper layer h ($d > h$) computed for a $\kappa = -0.98$ (in blue) and $\kappa = -0.998$ (in red) for ratios $r/d = 1$ and $h/d = 0.25$. It is also represented the potential relative error.

5 Conclusions

In this paper, we have revised the mathematical and numerical model for grounding analysis in two-layered soil models. Furthermore it has been presented for the first time a methodology for the acceleration of the convergence of the series involved in the computing of potential, which is the larger bottleneck in the computational cost of the numerical approach. Nowadays, we are working in the application of acceleration techniques in the computing of matrix coefficients of the LSE of the BEM approach.

Acknowledgments

This work has been partially supported by the "Ministerio de Educación y Ciencia" (grants #DPI2006-15275 and #DPI2007-61214) cofinanced with FEDER funds, by R&D projects of the "Xunta de Galicia" and the "Universidade da Coruña".

References

[1] IEEE Std.80, *IEEE Guide for safety in AC substation grounding.* New York, (2000).

[2] Sverak J.G., *Progress in step and touch voltage equations of ANSI/IEEE Std.80*, IEEE T. Power Delivery,**13**, 762–767, (1999).

[3] Garrett D.L., Pruitt J.G., *Problems encountered with the APM of analyzing substation grounding systems*, IEEE T. PAS **104**, 3586-3596, (1985).

[4] Navarrina F., Colominas I., Casteleiro M., Why do computer methods for grounding analysis produce anomalous results?, *IEEE T. Power Delivery* **18**, 1192-1202, (2003).

[5] Colominas I., Navarrina F., Casteleiro M., *A BE numerical approach for grounding grid computation*, Comp. Meth. App. Mech. Engrg., **174**, 73-90, (1999).

[6] Navarrina F., Colominas I., Casteleiro M., *Analytical integration techniques for earthing grid computation by BEM*, In "Numer. Meth. in Engrg and Appl. Sc.", 1197–1206, CIMNE, Barcelona, (1992).

[7] Colominas I., Gómez-Calviño J.,Navarrina F., Casteleiro M., *Computer analysis of earthing systems in horizontally and vertically layered soils*, Electric Power Systems Research, **59**, 149-156, (2001).

[8] Colominas I., Navarrina F., Casteleiro M. *A numerical formulation for grounding analysis in stratified soils*, IEEE T. Power Delivery, **17**, 587-595, (2002).

[9] Colominas I., *A CAD system of grounding grids for electrical installations: A numerical approach based on the Boundary Element integral method*, (in spanish), Ph.D. Thesis, Civil Engrg. Sch., Universidad de La Coruña, (1995).

[10] Banerjee P.K., *The BEM in engineering*, Mc Graw-Hill, London (1995).

[11] Johnson C., *Numerical solution of partial differential equations by the Finite Element Method*, Cambridge Univ. Press, Cambridge, USA, (1987).

[12] Tagg G.F., *Earth Resistances*, Pitman Pub. Co., New York, (1964).

[13] Sunde E.D., *Earth conduction effects in transmission systems*, McMillan, New York, (1968).

[14] Aneiros J., *Desarrollo de una Formulación Numérica para el Cálculo y Diseño de Tomas de Tierra de Subestaciones Eléctricas incorporando un Modelo de Terreno de Dos Capas*, Technical Project, Civil Engrg School, Universidade da Coruña (1996).